

# Heat Transfer Analysis in the Cooling Flume of a Single Droplet Evaporation Test Rig

Deqin Yuan, Xiaorong Wang\*, Zhihao Shen, Leisen Yuan, Hong Yang

Jiangsu University of Science and Technology, Zhenjiang, Jiangsu, 212003, China

Email: [49315273@qq.com](mailto:49315273@qq.com)

## Abstract

In order to study the cooling effect of flowing water on the axis of cooling flume in the single-droplet evaporating test rig, the thermal gas of the cooling axis of the flow water in the cooling flume is simulated. And the changes of gas temperature in the cooling flume is simulated. In this study, the mathematical model of gas-liquid two-phase flow heat transfer process was proposed and ANSYS FLUENT software was used. The cooling effects of cooling water with different mass flow rates on the air in the flume were also studied. The results show that the higher the mass flow rate is, the more obvious the cooling effect is when the gas velocity is 2m/s. The cooling flow rates have an optimum value, that is, the saturation value is 0.075 kg/s.

**Keywords:** cooling flume, cooling efficiency, optimum cooling flow rate, heat transfer

## 1. Introduction

The high efficiency combustion of internal combustion engine plays an important role in the further development of modern society. For this reason, a single droplet evaporation test rig has emerged. However, due to the droplets from the 10 mm test bed stomata into the cavity at the velocity of 300 mm/s, transmitted to the experimental observation position, the violent evaporation will make the experimental results have a great error in the temperature change process between 303K and 1073K. Therefore, the cooling flume is rather crucial in droplet evaporation experiment.

In this area of the cooling unit, Elsbett in Germany adopted the oil-cooling method in the 382TC diesel engine cooling system [1]. Compared with the traditional cooling method, the low-strength cooling mode and the multi-level folding structure slot model reduce the fuel consumption while increasing the cooling Media contact surface, and it's cooling efficiency increased by nearly 12% than ordinary devices. Germany's Siemens adopted the wind and water mixing cooling method in their research and development of SM150 frequency converter [2]. It was divided into three IGCT modules for further cooling, greatly improving the cooling efficiency. And Japan's Fuji Electric Co., Ltd. developed air-cooled cooling device mainly for cooling efficiency [3], carrying out the multi-level cooling by the refrigerant compressor and radiator, and increased the cooling efficiency of 16%. EGR coolers [4], on the other hand, use gas to cool, reducing the emission of harmful gases while reducing fuel consumption. In addition, the new energy cooling methods such as wind cooling due to its corrosively remains to be studied [5]. In this study, compared with the above high-efficiency cooling methods, the emphasis is cooling results. Moreover, the harmful gases released by oil cooling and the corrosiveness of wind and electricity are not conducive to the experimental process. Therefore, this experiment adopts the water cooling method which is moderate in cooling performance and innocuously green. What's more, taking into account the actual

device structure, the flume structure is added inside the cooling device to increase the cooling contact area to achieve adequate cooling.

Based on the definite cooling method and the mathematical model of gas-liquid two phase heat transfer inside the cooling flume. This paper focused on the influence of the axial water jet velocity on the axial and circumferential cooling uniformity of the cooling flume surface, to provide a reference and basis for the parameter selection in the actual production of control cooling equipment.

## 2. Mathematical model

The basic laws of physical conservation must follow the basic laws of physical conservation, including the law of conservation of mass, the law of conservation of momentum and the law of conservation of energy.

### 2.1. Momentum conservation equation

The law of conservation of momentum: the rate of change of the momentum of the fluid to the time in a microelement equals to the sum of the external forces acting on the microelement. Momentum conservation equation (N-S equation) is as follows:

$$\frac{\partial(\rho u)}{\partial x} + \text{div}(\rho u u) = \text{div}(\mu \text{grad} u) - \frac{\partial p}{\partial x} + S_u \quad (1)$$

$$\frac{\partial(\rho v)}{\partial x} + \text{div}(\rho v u) = \text{div}(\mu \text{grad} v) - \frac{\partial p}{\partial y} + S_v \quad (2)$$

$$\frac{\partial(\rho w)}{\partial x} + \text{div}(\rho w u) = \text{div}(\mu \text{grad} w) - \frac{\partial p}{\partial z} + S_w \quad (3)$$

Where,  $\mu$  represents the dynamic viscosity.  $p$  represents the pressure on a fluid microelement.  $S_u$ ,  $S_v$  and

$S_w$  are generalized sources of the conservation of momentum conservation equation.

### 2.2. Energy conservation equation

The law of conservation of energy: The increase of energy in the microelement equals to the work done by physical and surface forces to the microelements in the net heat flow of the microelement.

The energy conservation equation with the temperature  $T$  as the variable is as follows:

$$\frac{\partial(\rho T)}{\partial t} + \text{div}(\rho u T) = \text{div}\left(\frac{k}{c_p} \text{grad} T\right) - \frac{\partial p}{\partial y} + S_T \quad (4)$$

Where,  $C_p$  represents the specific heat capacity.  $T$  represents the temperature.  $k$  represents the heat transfer coefficient of the fluid.  $S_T$  represents the internal heat source of the fluid and the conversion of the mechanical energy of the viscous fluid into the heat energy.

### 2.3. The standard $k$ - $\epsilon$ model

The standard  $k$ - $\epsilon$  model is a semi empirical formula, mainly based on turbulent kinetic energy and diffusivity. The  $k$  model is a precise equation, and the  $\epsilon$  equation is an equation deduced form the empirical formula. The  $k$ - $\epsilon$  formula assumes that the flow field is completely turbulent, the viscosity among all the molecules can be ignored. Therefore, the standard  $k$ - $\epsilon$  model can only be applied to the turbulent flow field.

Here is the standard  $k-\varepsilon$  model, the turbulent TKE equation  $k$ , and the diffusivity equation is as follows:

$$\frac{\partial(\rho k)}{\partial t} + \frac{\partial(\rho k u_i)}{\partial x_i} = \frac{\partial}{\partial x_j} \left[ \left( \mu + \frac{\mu_t}{\sigma_k} \right) \frac{\partial \varepsilon}{\partial x_j} \right] + G_k + G_b - \rho \varepsilon - Y_M + S_k \quad (5)$$

$$\frac{\partial(\rho \varepsilon)}{\partial t} + \frac{\partial(\rho \varepsilon u_i)}{\partial x_i} = \frac{\partial}{\partial x_j} \left[ \left( \mu + \frac{\mu_t}{\sigma_k} \right) \frac{\partial \varepsilon}{\partial x_j} \right] + C_{k\varepsilon} \frac{\varepsilon}{k} (G_k + C_{3\varepsilon} G_b) - C_{2\varepsilon} \rho \frac{\varepsilon^2}{k} + S_\varepsilon - Y_M + S_\varepsilon \quad (6)$$

Where,  $G_k = \mu_t \left( \frac{\partial u_i}{\partial x_j} + \frac{\partial u_j}{\partial x_i} \right) \frac{\partial u_i}{\partial x_j}$ , is the source term of the TKE caused by the average speed grade;

$G_b = \beta g_i \frac{\mu_t}{Pr_t} \frac{\partial T}{\partial x_i}$ , is the source term of the TKE caused by the buoyant force,  $g_i$  is the part of gravity constant on the  $i$  direction.  $Pr_t$  is the Prandtl number of the turbulent flow  $Y_M = 2\rho \varepsilon M_t^2$ , which represents the pulsation dilatation of the compressible turbulent flow,  $M_t$  is the Mach number of the turbulent flow.  $\sigma_k$  and  $\sigma_\varepsilon$  are the Prandtl numbers of the TKE  $k$  and the dissipation rating  $\varepsilon$ .  $C_{1\varepsilon}, C_{2\varepsilon}$  and  $C_{3\varepsilon}$  are the empirical constants.  $S_k$  and  $S_\varepsilon$  are the source term defined by the users.

The quasi- $k-\varepsilon$  model is based on the  $k-\varepsilon$  model, it is modified for the low Reynolds number, the compressibility and the shear flow propagation. One of form change of the standard  $k-\varepsilon$  model is the SST  $k-\omega$  model, and it can be used in the Fluent. The applied scope: the  $k-\omega$  model predicted the propagation velocity of the free shear flows, like the wake flow, the mixing flow, the flat-plate flow, the circular cylinder and the radial injection, therefore it applies the wall-bounded flow and the free shear flow.

### 3. Physical model

Fig. 1 shows simplified geometric simplification of cooling flumes (two dimensions). Three-dimensional model of the entire unit is the cylindrical model rotated into on symmetry axis of the basin 1, so the entire model is a cylinder, geometric figure composed of basin 1 is a frustum of a cone, the large spatial cylindrical turns into the basin 2 and the basin 3 after removing the frustum of a cone.

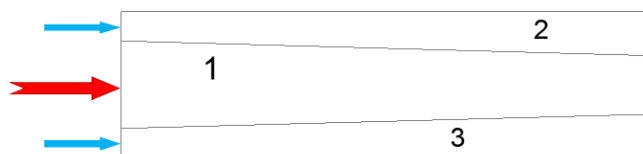


Fig. 1. Simplified geometric model

The basin 2 and the basin 3 are the cold water basins, the entrance is the direction marked by the blue arrow, and the outlet is the opposite direction. as the same times, the basin 1 is the hot air basin, the entrance is the direction marked by the red arrow, the outlet is the opposite direction. According to the actual measurement, under the conditions of this experiment, the hot air will flow into the hole at 2m/s and the equivalent mass flow rate is 0.000165 kg/s.

In addition, the basin 2 and the basin 3 in the periphery contact atmospheric environment through

outer boundary contact, because the water is cold, so medium in the basin 2 and the basin 3 will not exchange heat with the outside world, therefore in the simulation, the boundary between the basin 2, 3 and the external environment is set up as adiabatic wall. In this study, the heat exchange is mainly the cooling effect of the water in the basin 2 and the basin 3, so it is important to set the boundary of the basin 1 and the basin 2, 3 as the heat exchange wall.

The inlet diameter of the basin 1 is  $18\text{ mm}$ , the outlet diameter of basin 1 is  $10\text{ mm}$ , and the diameter of the circle formed by the boundary of the basin 2 and basin 3 is  $30\text{ mm}$ , which is the geometric parameter of the model.

To sum up, set the three drainage basins as entrance to the quality flow, and the outlet is set as the pressure outlet.

The experiment study the temperature distribution of the velocity of the cold water on the axis in this structure, so the control variable of the experiment is the velocity of the cold water. Therefore, the simulation controls other variables unchanged, and adjusts the water flow velocity to discuss the temperature distribution of the analysis axis. In the structure analysis model, select the mass flow rate of  $0.01\text{ kg/s}$ ,  $0.025\text{ kg/s}$ ,  $0.05\text{ kg/s}$ ,  $0.075\text{ kg/s}$ ,  $0.1\text{ kg/s}$  to study the temperature distribution of the axis in the structure.

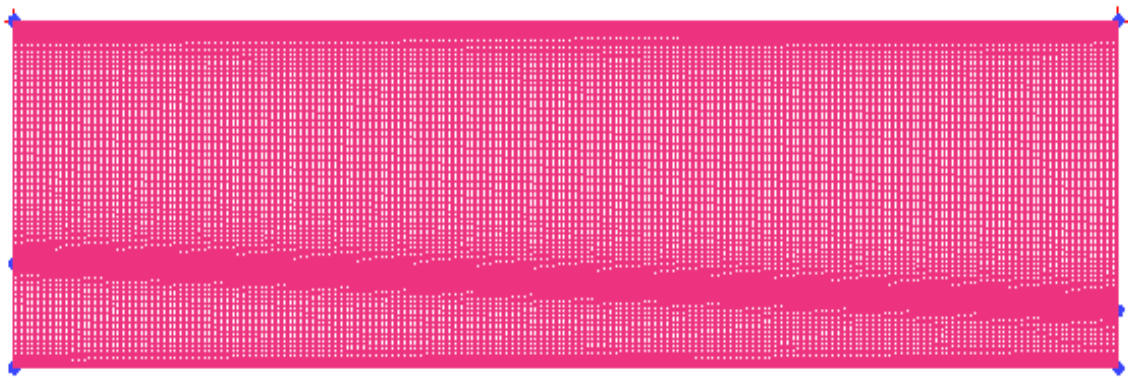


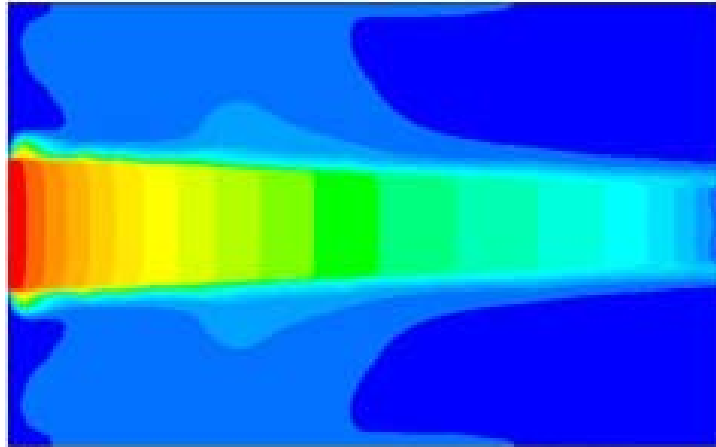
**Fig.2.**grid maked by ICEM CFD

This is grid maked by ICEM CFD. And the number of his grids is around 30 thousand.

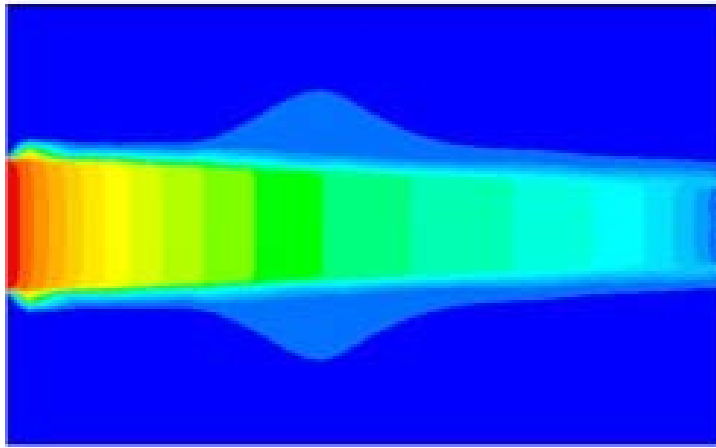
## 4. Results and discussion

### 4.1. Cooling effects of different mass flow rates of water

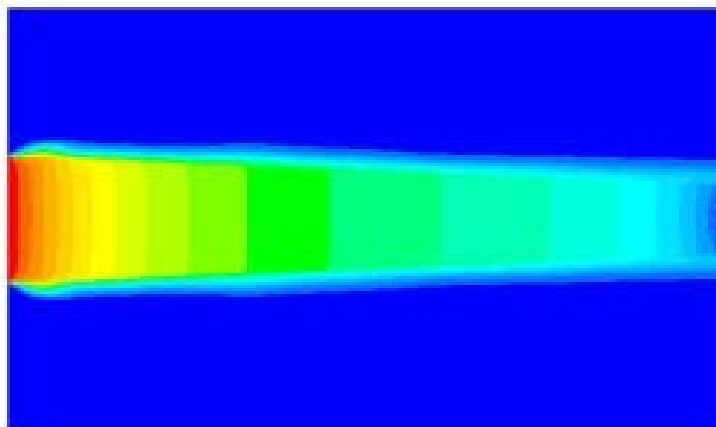
Figure 2 is the simulation of the high temperature entrance of the single-droplet evaporation test rig under cooled water conditions. According to the simulation results, the highest temperature measured by simulation at different cooling rates is the hot gas inlet temperature  $1073\text{ K}$  and the lowest temperature is the hot gas outlet temperature that roughly swings at  $380\text{ K}$  ( $107\text{ }^{\circ}\text{C}$ ). Analysis of the trend of symmetry axis temperature changes shows that with the measurement location promoted from the hot air outlet to the entrance, the cooling effect continues to increase, the hot air temperature continues to decrease, and the maximum cooling rate can reach the effect of above  $600\text{ K}$ .



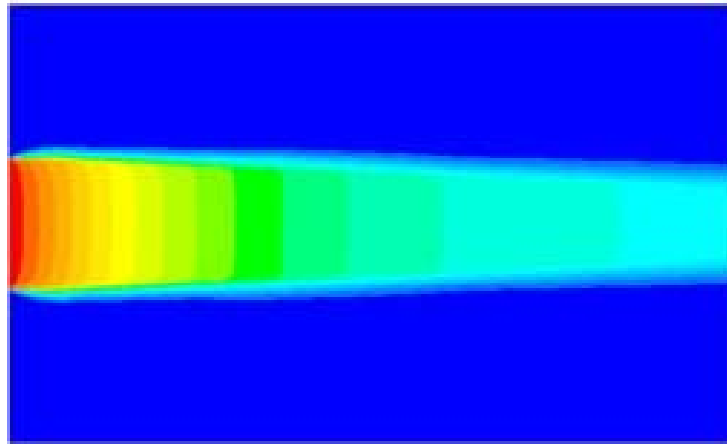
**a).** mass flow rate  $0.01 \text{ kg/s}$



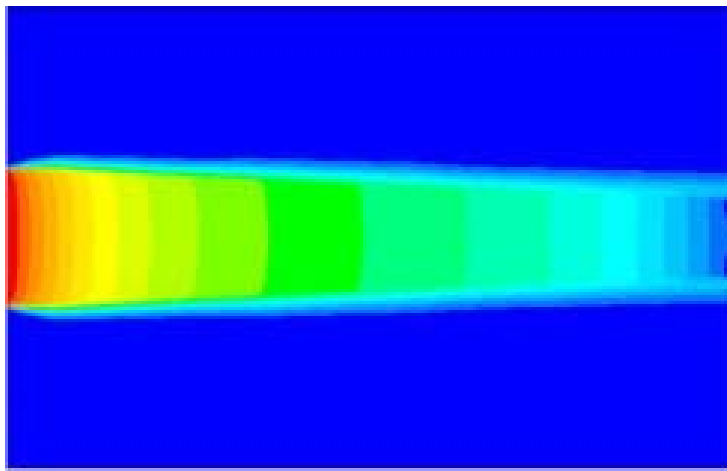
**b).** mass flow rate  $0.025 \text{ g/s}$



**c).** mass flow rate  $0.05 \text{ kg/s}$



d). mass flow rate  $0.075 \text{ kg/s}$



e). mass flow rate  $0.1 \text{ kg/s}$

**Fig.3.** Temperature distribution in the cooling flume

#### 4.2. Temperature variation of the axis in the cooling flume

As shown in Fig. 3, the temperature distribution at the axis where the mass flow rates are  $0.05 \text{ kg/s}$ ,  $0.075 \text{ kg/s}$  and  $0.1 \text{ kg/s}$  is extracted ( $x$  is the distance to the gas inlet) and comparatively analyzed. The mass flow rate of  $0.075 \text{ kg/s}$  is obviously better than  $0.05 \text{ kg/s}$ . The cooling differences are mainly reflected in the middle section and the difference of cooling on both sides is not obvious. According to the data analysis, the maximum temperature from the proximal inlet is basically the same, which is due to the impact of single droplet evaporation test rig cavity environment, and the lowest temperature from the proximal outlet is basically the same because the cooling has reached the saturation effect (basically identical to the water temperature), unable to carry out heat exchange. Remove inlet and outlet, due to differences in heat transfer produced by different water velocity mainly occurs in the middle section, the middle segment is mainly analyzed. According to the Fig. 3, it is found that while the mass flow rate of water is increased from  $0.05 \text{ kg/s}$  to  $0.075 \text{ kg/s}$ , the highest temperature difference can reach  $400 \text{ k}$  in the same location.

Secondly, the temperature distribution ( $x$  is the distance from the inlet of the gas) at the axis where the mass flow rates are  $0.075 \text{ kg/s}$  and  $0.1 \text{ kg/s}$  is analyzed. By the comparative analysis, the two curves are basically the same and the cooling effect of water at the mass flow rate of  $0.1 \text{ kg/s}$  is better than the one at

the mass flow rate of  $0.075 \text{ kg/s}$  in the initial state of cooling. However, the two curves near the exit appear differences due to the environmental impact but basically the same. From this analysis, the section from  $0.075 \text{ kg/s}$  increased to  $0.1 \text{ kg/s}$  has reached the cooling saturation and no more significant heat transfer differences can be formed by increasing the water velocity.

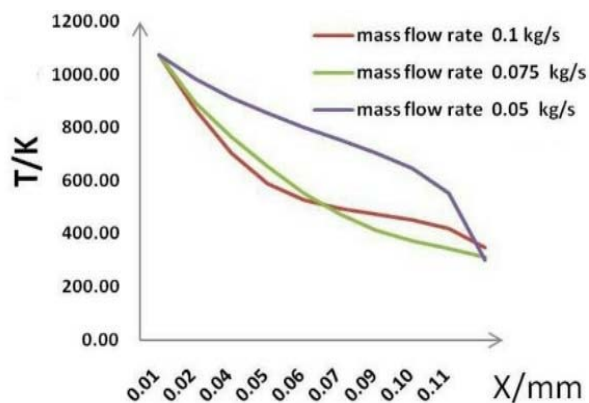


Fig.4. temperature variation curve of cooling flume axis

## 5. Conclusions

Within the mass flow rate ranging from  $0.01 \text{ kg/s}$  to  $0.1 \text{ kg/s}$ , Water can completely cool the  $1073 \text{ K}$  gas to about  $330 \text{ K}$  to achieve cooling effect.

The cooling effect will vary at different water velocities. So the cooling water volume is an important factor that affects the heat transfer. When the gas flow and temperature are constant, there is an optimum cooling mass flow rate. Under the simulated conditions, the mass flow of cold water should be controlled at about  $0.075 \text{ kg/s}$ . The cooling effect is not good if the mass flow is more or less.

## References

- [1] Shengji Liu. Performance and Construction Features of New Model 382TC Oil - Cooled DI Diesel Engine. Chinese Internal Combustion Engine Engineering, 2009, 17(1): 70-77.
- [2] Enhui Zhou. Analysis of the damage cause of the phase module of the SIEMENS SM150 medium voltage inverter. Electrical World, 2014, 55(9).
- [3] Eizan Rino. Cooling System. 2017.
- [4] Jiandong Wang. Analysis of EGR cooler technology and manufacturing process. Auto Time, 2016, 4:44-45.
- [5] Jie Dai. Research and development of coolant for wind power cooling device. Guangdong chemical industry, 2017, 11:150-151.
- [6] Xiaodan Liu. Numerical analysis of the flow of water jacket coolant in gasoline engine. Jilin, College of automotive engineering, Jilin University. 2009. 9-14.